Anisotropic optical conductivity of $Sr_3Ru_2O_7$

C. Mirri,[1] L. Baldassarre,[1] S. Lupi,[1] M. Ortolani,[2] R. Fittipaldi,[3] A. Vecchione,[3] and P. Calvani[1]
[1]*Dipartimento di Fisica and CNR-INFM "Coherentia," Università di Roma La Sapienza, Piazzale A. Moro, 2, I-00185 Roma, Italy*
[2]*Berliner Elektronenspeicherring-Gesellschaft für Synchrotronstrahlung m.b.H., Albert-Einstein Strasse 15, D-12489 Berlin, Germany*
[3]*Dipartimento di Fisica "E. R. Caianiello", Università di Salerno and CNR-INFM Laboratorio Regionale Supermat, Via S. Allende, I-84081 Baronissi Salerno, Italy*
(Received 30 May 2008; published 31 October 2008)

The optical conductivity $\sigma(\omega)$ of $Sr_3Ru_2O_7$ has been studied both in the *ab* planes, between 12 and 450 K, and along the *c* axis between 12 and 300 K. $\sigma_{ab}(\omega)$ is Drude-type but, for increasing *T*, it shows a crossover around 300 K to a regime with enhanced scattering rate, probably driven by a stronger coupling with the optical phonons. The spectral weight shows the imprints of strong correlations, but less pronounced than in a high-T_c material. Along the *c* axis, the Drude term has a much smaller plasma frequency, and a strong absorption appears at 1 eV. These findings indicate an anisotropic metallic state where electron-electron and electron-phonon interactions play a major role. This picture may be reconciled with the local-density calculations reported in the literature, which predict an insulating *c* axis, once those interactions are taken into account.

DOI: 10.1103/PhysRevB.78.155132 PACS number(s): 74.70.Pq, 78.30.−j, 78.20.−e

I. INTRODUCTION

The Ruddlesden-Popper-type series $Sr_{n+1}Ru_nO_{3n+1}$ ($n=1,2$, and ∞) has attracted wide interest in the last decade due either to the unconventional superconductivity of Sr_2RuO_4 ($n=1$), where the Cooper pairs are in a *p*-symmetry triplet state,[1] or to the metamagnetism and quantum criticality shown by $Sr_3Ru_2O_7$ ($n=2$) at $T \lesssim 1$ K.[2,3] In turn, $SrRuO_3$ ($n=\infty$) is the only ferromagnetic material among the itinerant 4*d* transition-metal oxides.[4] In the present paper we focus on the double-layered, nonsuperconducting, perovskite $Sr_3Ru_2O_7$, with the aim to investigate its basically unexplored, anisotropic, optical properties. The interest for anisotropic, conducting oxides has grown in recent years after the discovery of high-T_c superconductivity in the cuprates, which share with the ruthenates the perovskite structure and the typical transition metal-oxygen layer. Moreover, single crystals, large and pure enough along different axes, have been grown successfully for many chemical compositions, allowing for a detailed determination of their anisotropic behavior by different spectroscopic techniques.

$Sr_3Ru_2O_7$ has a quasitetragonal cell elongated along the *c* axis. In the calculations of both electronic and phonon bands, a symmetry $I4/mmm$ is generally assumed. However, under rotations of the RuO_6 octahedra around the *c* axis, such structure tends to transform into lower-symmetry orthorhombic phases like *Bbcb* (no. 68).[5] At room temperature, the average values for the lattice constants of the tetragonal cell are $\langle a \rangle = (a+b)/2 = 0.5500$ nm (with $a<b$), and $c=2.0725$ nm. At 40 K $a=b$, and below this temperature $a>b$.[5] The octahedra RuO_6 are formed by the hybridized bonds between the 2*p* levels of oxygen and the 4*d* levels of Ru^{4+}, which host four electrons. In the crystal field these orbitals are split by an energy[6] $10Dq$, into a triplet t_{2g} and a doublet e_g. In $Sr_3Ru_2O_7$, the crystal field is strong enough that $10Dq > J$, where *J* is the Hund energy. Therefore, in the ground state the four electrons are in the t_{2g} state, e_g is empty, and the total spin *S* is 1. In turn, the degeneracy of the t_{2g} state is removed by the Jahn-Teller distortion.

In $Sr_3Ru_2O_7$ the carriers are holes, as shown by Hall data.[7] The resistivity is anisotropic, consistently with the quasi-two-dimensional Fermi surface extracted from band-structure calculations.[8] Indeed, both the *ab* plane resistivity $\rho_{ab}(T)$ and that along *c*, $\rho_c(T)$, are metallic. However, at 300 K $\rho_c(T) \sim 40\rho_{ab}(T)$.[9] This latter is linear down to 15 K, while[10] $\rho_{ab}(T) \propto T^{1.5}$ between 15 and 6 K, $\propto T^2$ below 6 K. This change in slope, which is much more pronounced in $\rho_c(T)$, corresponds to a peak in the magnetic susceptibility at 16 K which was tentatively interpreted in terms of ferromagnetic fluctuations.[9] A ferromagnetic phase is observed only under external pressure, with a Curie temperature $T_c \simeq 70$ K at 1.1 GPa.[11]

Concerning the optical properties, those of[12,13] Sr_2RuO_4 and of[14] $SrRuO_3$ have been studied in detail, while for $Sr_3Ru_2O_7$ only the room-temperature optical conductivity $\sigma_{ab}(\omega)$ of the *ab* plane can be found in the literature.[15,16] $\sigma_{ab}(\omega)$ appears metallic in the midinfrared and shows electronic bands above 3 eV, which are attributed to charge-transfer (CT) transitions between the O 2*p* and the Ru t_{2g} levels. Spectra at lower temperatures were reported only in the region of the stretching mode of the Ru-O bond, to study how its peak frequency depends on *T*.

The present experiment is aimed at completing our optical knowledge of $Sr_3Ru_2O_7$, by measuring its $\sigma(\omega)$ both with the radiation field polarized in the *ab* plane (between 12 and 450 K) and along the *c* axis (between 12 and 300 K), for ω ranging from the far infrared to the near UV.

II. SAMPLE AND EXPERIMENT

The $Sr_3Ru_2O_7$ single crystal was grown by the floating zone technique and characterized by x-ray diffraction and scanning electron microscopy. Traces of the $Sr_4Ru_3O_{10}$ phase, as usual in these samples, were found. The reflectivity $R(\omega)$ of the crystal was measured at nearly normal incidence

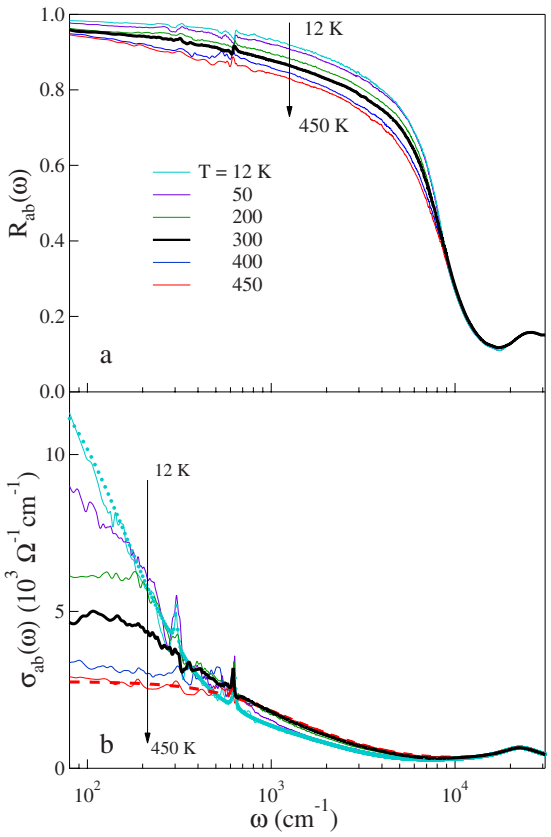

FIG. 1. (Color online) Reflectivity (a) and optical conductivity (b) of the *ab* plane of $Sr_3Ru_2O_7$ at selected temperatures between 12 and 450 K. In (b), fits to a Drude-Lorentz model (see text) are shown for the highest (dotted line) and the lowest temperature (dashed line).

(8°) at different temperatures, both with the field polarized in the *ab* plane and along the *c* axis. The reference was obtained by evaporating a gold film onto the sample itself in the far and midinfrared, a silver film in the near infrared and the visible range. Data were collected by a rapid-scanning interferometer from 80 (*ab* plane) or 60 (*c* axis) to 20 000 cm^{-1}, and by thermoregulating the samples within ±2 K at ten temperatures between 12 and 450 K. The spectra were then extended at room temperature up to 30 000 cm^{-1} by using a monochromator and an aluminum film as reference. The optical conductivity $\sigma(\omega)$ was extracted from the corresponding reflectivity curves by use of standard Kramers-Kronig transformations. In the *ab*-plane measurements, in order to exclude the presence of spurious contributions from the less-metallic *c* axis due to small errors in cutting the crystal,[17] the polarizer was rotated until the maximum reflectivity was attained at room temperature. This ensured that the field was aligned orthogonally to the slope of any possible, residual miscut.

III. RESULTS AND DISCUSSION

A. Optical conductivity of the *ab* plane

The *ab* plane reflectivity $R_{ab}(\omega)$ of $Sr_3Ru_2O_7$, as measured from 12–450 K and from 80–30 000 cm^{-1}, is shown in Fig. 1(a). $R_{ab}(\omega)$ increases, as T is lowered, up to 10 000 cm^{-1}. The plasma edge at ~12 000 cm^{-1} indicates that the system is a good metal. The optical conductivity $\sigma_{ab}(\omega)$ extracted from $R_{ab}(\omega)$ through the Kramers-Kronig transformations is shown in Fig. 1(b). It is basically Drude-type, as confirmed by the fits to a Drude-Lorentz model shown in the figure for the highest (450 K) and the lowest temperature (12 K). The plasma frequency ω_{pD} turns out to be 12 000 cm^{-1}, independent of temperature. $\sigma_{ab}(\omega)$ does not show any feature similar to the pseudogap observed[18] below 200 cm^{-1} and 50 K in $Ca_3Ru_2O_7$. This confirms that, unlike the latter compound, $Sr_3Ru_2O_7$ does not present charge/spin density wave instabilities down to the lowest temperature here investigated. The extrapolated value $\sigma_{ab}(\omega \to 0)$ at 300 K, 5000 Ω^{-1} cm^{-1}, is in excellent agreement with the dc determination $\sigma_{ab}(0)$ reported in Ref. 9 (4800 Ω^{-1} cm^{-1}). However, as T lowers below 100 K, the extrapolated value $\sigma_{ab}(\omega \to 0)$ increases less rapidly than the dc conductivity. This discrepancy may be due to the lack of data below 80 cm^{-1}, which produces an increasing error as the Drude term becomes narrower.

An interesting quantity is the relaxation rate of the carriers Γ. In Fig. 2(a) it is plotted versus temperature as obtained from the above Drude fit. Below 50 K, Γ drops as reported for the dc resistivity,[9] while at higher T it clearly shows two different regimes, with a crossover around room temperature. Above 300 K, Γ decreases for decreasing T much more rapidly than between room temperature and 50 K. Figure 2(b) shows instead the frequency-dependent relaxation rate $\Gamma(\omega)$ that one can extract from the dielectric function $\tilde{\epsilon}(\omega) = \epsilon_1(\omega) + i\epsilon_2(\omega)$ in the framework of an extended Drude model,[19]

$$\Gamma(\omega) = \frac{(\omega_{pD}^2/\omega)\epsilon_2(\omega)}{\{[\epsilon_1(\omega) - \epsilon_\infty]^2 + \epsilon_2^2(\omega)\}^2}. \quad (1)$$

One may first remark that $\Gamma(\omega \to 0)$ in Fig. 2(b) is consistent at all temperatures with the $\Gamma(T)$ of Fig. 2(a), within the errors involved in Eq. (1). Moreover, the existence of two regimes with a crossover at room temperature is confirmed and further information is added. Indeed in Fig. 2(b) at 12 K, if one neglects the phonon contributions, Γ versus ω follows an exactly linear increase (dashed line) up to 1500 cm^{-1}. A linear $\Gamma(\omega)$ has been often observed in cuprates with a strongly metallic character.[20] The same slope is conserved in Fig. 2(b) up to 300 K, while deviations are detected at 350 K and, much stronger, at 450 K. They consist of an excess of relaxation rate at low frequency, in the region of the longitudinal and transverse optical phonons. This unusual behavior is just opposite to that reported in the *ab* plane of the underdoped cuprates for a pseudogap Δ_p. Therein, since no suppression of spectral weight is observed directly in $\sigma_{ab}(\omega)$, some authors report a depletion[19] in $\Gamma(\omega)$ for $\omega < \Delta_p$ and $T < T^*$, the pseudogap temperature. This is interpreted as a suppression of certain scattering channels for $T < T^*$. Here, the low-ω increase in Γ in Fig. 2(b) for $T > 300$ K associated with the change in slope in Fig. 2(a) points toward an enhanced interaction of the holes with the optical phonons.

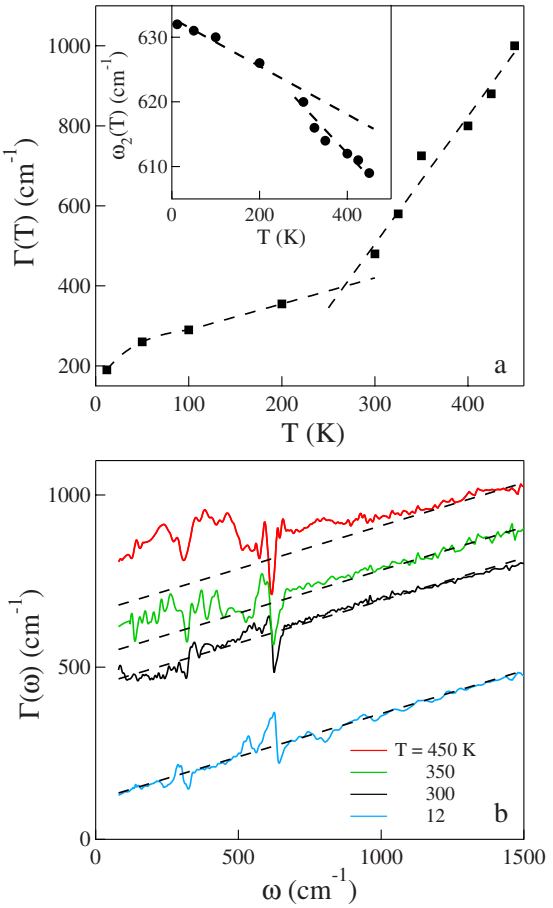

FIG. 2. (Color online) (a) Free-carrier relaxation rate Γ versus T in the ab plane, as obtained from a conventional Drude fit. In the inset, the frequency ω_2 of the in-plane stretching mode is also reported versus T. (b) Γ plotted versus ω at four temperatures, as calculated from Eq. (1) in the framework of an extended Drude model. In all sets of data, the dashed line is the best linear fit to $\Gamma(\omega)$ at 12 K.

This finding is further supported in the inset of Fig. 2(a), which reports the T dependence of ω_2, the peak frequency of the in-plane Ru-O stretching mode. At 300 K and below, the data are in agreement with those reported in Ref. 16. In the same range of temperatures where both the conventional Drude $\Gamma(T)$ and the extended Drude $\Gamma(\omega)$ undergo a crossover between different regimes, also $\omega_2(T)$ exhibits a change in slope. This may indicate either a structural phase transition which affects both the carriers and the phonon, or a strong coupling between the carriers and the optical stretching mode, which, at $T>300$ K, enhances the usual softening produced by lattice expansion. As diffraction data on $Sr_3Ru_2O_7$ are available only for $T\leq 300$ K, this remains an open question.

One can now shortly describe the other features which appear in Fig. 1(b). If, alternatively to the extended Drude model, one uses a Drude-Lorentz fit, one should add to the Drude term a broad midinfrared oscillator peaked at 1500 cm^{-1}. In the far infrared, in addition to the stretching at ω_2, below 100 K another transverse optical mode emerges at ω_1 from the Drude continuum. It can be assigned to a bending of the Ru-O square lattice. One finds $\omega_1=307$, 303, and 299 cm^{-1} at 100, 50, and 12 K, respectively. In the same range of temperatures the ab plane undergoes the already mentioned distortion, with[5] $2(b-a)/(b+a)$ switching from $+0.6\times10^{-3}$ at 100 K to -0.4×10^{-3} at 12 K. Finally, in the visible range the best fit to $\sigma_{ab}(\omega)$ requires the band at 23 000 cm^{-1} assigned in Ref. 16 to the CT transitions between the O $2p$ and the Ru t_{2g} levels.

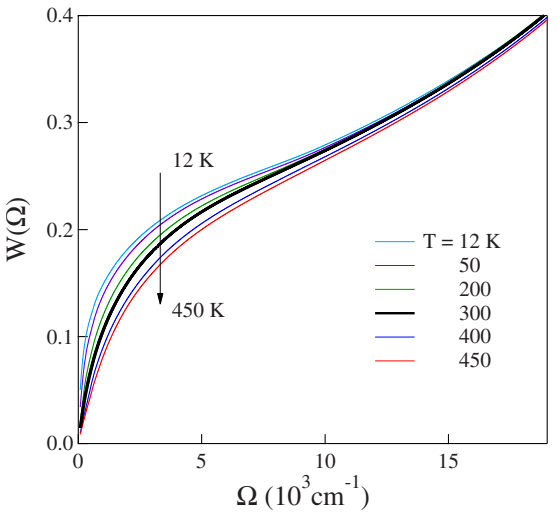

FIG. 3. (Color online) Spectral weight of $Sr_3Ru_2O_7$ in the ab plane versus the cut-off frequency in Eq. (2), at selected temperatures between 12 and 450 K.

B. Spectral weight in the *ab* plane

From the ab-plane optical conductivity of $Sr_3Ru_2O_7$ one can also calculate the spectral weight

$$W(\Omega,T)=\frac{2m^*V}{\pi e^2}\int_0^{\Omega}\sigma_{ab}(\omega,T)d\omega, \qquad (2)$$

where m^* is the effective mass of the carriers (here assumed to be equal to the free electron mass) and V is the volume of the formula-unit cell. The resulting W is plotted in Fig. 3 versus the cut-off frequency Ω at different temperatures. The f-sum rule on W establishes that all those curves collapse into a single one for $\Omega\to\infty$. However, a restricted sum rule is verified in conventional metals, according to which W becomes independent of T for $\Omega\sim\Omega_p$. Here Ω_p is the plasma edge, namely the Drude plasma frequency ω_{pD} renormalized by the screening effect of the higher-energy bound charges. For example, such sum rule is well verified in gold. On the contrary, in the ab plane of high-T_c cuprates the f-sum rule is not fulfilled, unless[21] $\Omega\gg\Omega_p$. This anomaly has been attributed to the effect of strong correlations, which act to mix the high- and low-energy scales in the optical response of the carriers.[22]

Both in conventional metals and in a superconducting cuprate such as $La_{2-x}Sr_xCuO_4$, moreover, the spectral weight depends on temperature as[21]

$$W(\Omega,T)=W_0[1-b(\Omega)T^2]. \qquad (3)$$

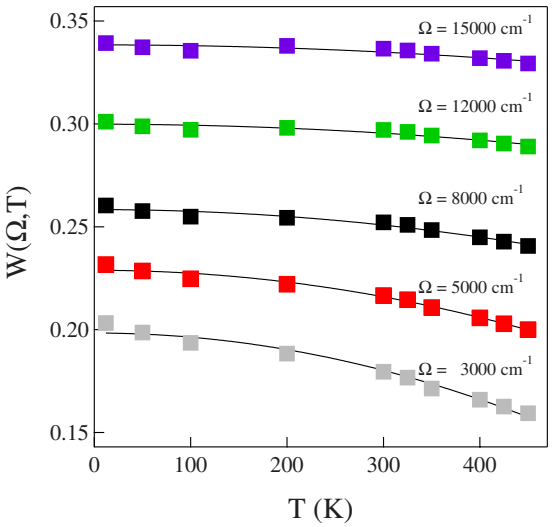

FIG. 4. (Color online) $W(\Omega)$ versus T for different Ω. The solid lines are fits to the quadratic form of Eq. (3).

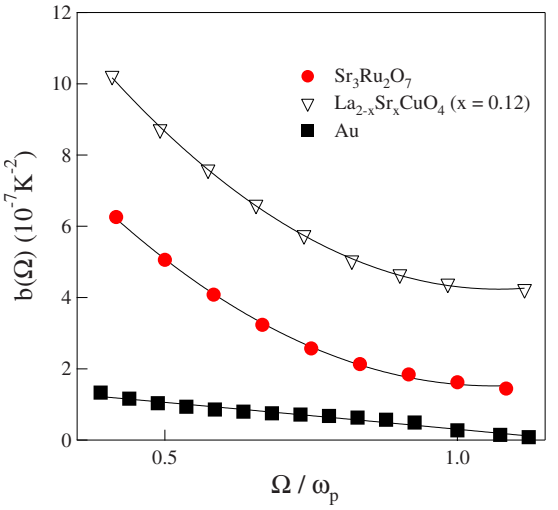

FIG. 5. (Color online) The coefficient $b(\Omega)$ of $Sr_3Ru_2O_7$ from Fig. 4, compared with that of gold and of the superconducting cuprate $La_{1.88}Sr_{0.12}CuO_4$. Data are reported versus a cut-off frequency Ω normalized to the plasma edge Ω_p of each compound. The lines are guides for the eyes.

The above quadratic dependence is expected on the basis of a one-band tight-binding model and of a Sommerfeld expansion of the kinetic energy. However, while in a conventional metal like gold W_0 and b are controlled by the same energy scale, namely the hopping rate t, in correlated oxides the former scale is larger by 1 order of magnitude than that which controls the frequency-dependent coefficient b which describes the "thermal response" of the carriers. Figure 4 shows $W(\Omega)$ versus T at different Ω, with the corresponding fits to Eq. (3). For increasing cut-off frequencies, the variation with T of W becomes weaker and weaker, but it is always larger than the experimental error. This latter is small, either as the reflectivity above room temperature is not affected by traces of water condensation, or as we evaporated gold at each T in order to compensate for any misalignment of the system due temperature variations.

Given the good agreement at any Ω, one can extract from the fits $b(\Omega)$. This quantity is plotted in Fig. 5 for $Sr_3Ru_2O_7$, and compared therein with that of gold and of the superconducting cuprate $La_{1.88}Sr_{0.12}CuO_4$. In order to facilitate the comparison, $b(\Omega)$ is reported versus Ω/Ω_p, where Ω_p is the plasma edge of each compound: 12 000, 21 500, and 6800 cm^{-1},[21] respectively.

In correlated materials, unlike in a conventional Fermi liquid, $b(\Omega)$ is appreciably different from zero well beyond the plasma edge,[21,22] while in a conventional metal like gold $b(\Omega) \simeq 0$ at Ω_p. Figure 5 shows that in $Sr_3Ru_2O_7$ $b(\Omega)$ behaves like the cuprate, even if its absolute values below Ω_p are intermediate between those of the cuprate and those of gold. Therefore, from the present analysis of the T dependence of the spectral weight one may conclude that in $Sr_3Ru_2O_7$ the effect of electron correlations is present but less pronounced than in the prototypical superconducting cuprate $La_{2-x}Sr_xCuO_4$.

C. Optical conductivity of the *c* axis

The reflectivity $R_c(\omega)$ of $Sr_3Ru_2O_7$, as measured with the radiation field polarized along the c axis from 12 to 300 K, is shown in Fig. 6(a). At 300 K and below 1200 cm^{-1} it is consistent with that of $Ca_3Ru_2O_7$ in Ref. 15. Except for the charge-transfer band at the highest frequencies, it looks quite

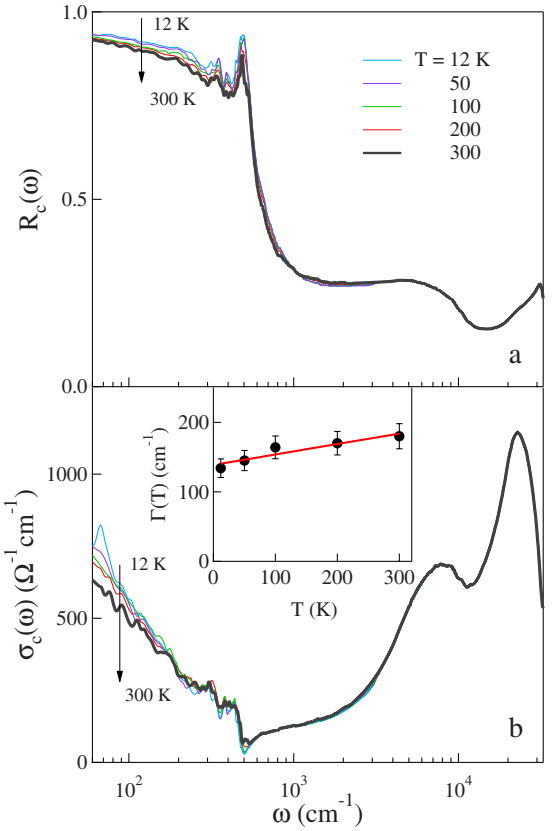

FIG. 6. (Color online) Reflectivity (a) and optical conductivity (b) of $Sr_3Ru_2O_7$, as measured with the field polarized along the c axis at selected temperatures between 12 and 300 K. The inset shows the width Γ versus T, provided by a conventional Drude fit to the far-infrared data.

different from that of the *ab* plane in Fig. 1(a). The plasma edge here falls at ~800 cm^{-1} (0.1 eV) and a strong absorption, not observed in the conductivity of the *ab* plane, appears in the near infrared. The separation between the two bands emerges clearly in the optical conductivity $\sigma_c(\omega)$ of Fig. 6(b). Therein, a Drude-Lorentz fit provides a plasma frequency $\omega_{pD}=2700$ cm^{-1}, independent of T within errors, and the relaxation rate $\Gamma(T)$ which is plotted in the inset. As a consequence, the extrapolated value $\sigma_c(\omega\rightarrow 0)$ at 300 K is 650 $\Omega^{-1}\,cm^{-1}$, much larger than the dc value $\sigma_c(0)=120$ $\Omega^{-1}\,cm^{-1}$ reported in Ref. 9. Similarly, $\sigma_c(\omega\rightarrow 0)$ does not show the strong increase in σ_{dc} reported therein below 50 K. These discrepancies might be explained by assuming an anomaly in $\sigma_c(\omega)$ at frequencies lower than those explored here, even if there are no hints to support such possibility at this stage. In the far infrared, three phonon lines are also detected, at peak frequencies 306, 382, and 440 cm^{-1}, independent of temperature within errors.

The above results can be compared with the band calculations reported in Ref. 8, which are based on a full-potential linearized augmented plane-wave method within a local-density approach. Along the direction Λ of the $\vec{k}$ space, which corresponds to the *c* axis in real space, they show a band (*A*) well below the Fermi level at E_F, and a flat band (*B*) at ~0.1 eV above E_F. Therefore this scheme describes an insulating *c* axis, in contrast with the present experiment. The apparent metallic behavior of the *c*-axis conductivity suggests that the band *B* is shifted from the calculated value toward lower energies by at least 0.1 eV, so that it crosses the Fermi energy. Such discrepancy may be attributed to the electron-electron and/or the electron-phonon interactions, not included, or only partially included, in local-density calculations. Both those effects have been here shown to be important in $Sr_3Ru_2O_7$.

If one assumes that band *B* crosses the Fermi level, one may fully reconcile the theory with the experimental result of Fig. 6(b). Indeed, the low dispersion of *B* implies a high effective mass of the carriers m^* and explains why, in the conductivity of the *c* axis, $\omega_{pD}^2=ne^2/m^*$ is smaller by a factor of 20 than in the *ab* plane. Moreover, if band *B* is occupied, also the strong near-infrared absorption in Fig. 6(b) has a natural explanation. Indeed, above E_F another band *C* is predicted,[8] about ~1 eV above *B*. The band at 8000 cm^{-1} can then be reasonably assigned to the interband transitions $B\rightarrow C$.

CONCLUSION

In the present paper we have studied the optical conductivity of *c*, both in the *ab* plane and along the *c* axis. $\sigma_{ab}(\omega)$ is metallic, with a plasma frequency which falls in the near infrared. The relaxation rate Γ increases linearly with T between 50 and 450 K, but shows a pronounced change in slope around room temperature. By studying the ω dependence of Γ in an extended Drude model, that crossover can be associated with an enhanced scattering rate above 300 K in the optical phonon frequency range, just opposite to the reported opening of a pseudogap in the $\Gamma(\omega)$ of certain underdoped cuprates. Around 300 K, also the T dependence of the stretching mode peak frequency shows an anomaly. Up to 450 K, the behavior with temperature of the spectral weight $W(\Omega,T)\propto\int_0^\Omega\sigma_{ab}(\omega)d\omega$ is quadratic, as observed both in conventional metals and in most cuprates. Its dependence on Ω is instead intermediate between that of a conventional metal and that of a highly correlated material like the high-T_c superconductor $La_{2-x}Sr_xCuO_4$.

When polarizing the field orthogonally to the *ab* plane, the conductivity changes sharply: the Drude term along the *c* axis has a much smaller plasma frequency, indicating a strong enhancement in the effective mass, and a broad absorption appears at 1 eV. According to the predictions of local-density calculations reported in the literature, a quasiflat band is close to the Fermi energy, and a dispersive band is placed at ~1 eV above that band. This structure is consistent with our results, provided that the flat band crosses the Fermi level instead of being empty as predicted. The inclusion of the interactions here shown to be important in $Sr_3Ru_2O_7$ might shift the band energies thus reconciling theory and experiment. Indeed, this double-layer ruthenate is here confirmed to be a strongly anisotropic metal with a rather weak interplane hopping, but cannot be described as a two-dimensional conductor like the high-T_c cuprates, where the *c* axis is insulating at any $T>T_c$.

[1] A. P. Mackenzie and Y. Maeno, Rev. Mod. Phys. **75**, 657 (2003), and references therein.
[2] A. G. Green, S. A. Grigera, R. A. Borzi, A. P. Mackenzie, R. S. Perry, and B. D. Simons, Phys. Rev. Lett. **95**, 086402 (2005), and references therein.
[3] A. Tamai, M. P. Allan, J. F. Mercure, W. Meevasana, R. Dunkel, D. H. Lu, R. S. Perry, A. P. Mackenzie, D. J. Singh, Z.-X. Shen, and F. Baumberger, Phys. Rev. Lett. **101**, 026407 (2008).
[4] L. Klein, J. S. Dodge, C. H. Ahn, G. J. Snyder, T. H. Geballe, M. R. Beasley, and A. Kapitulnik, Phys. Rev. Lett. **77**, 2774 (1996).
[5] H. Shaked, J. D. Jorgensen, S. Short, O. Chmaissem, S.-I. Ikeda, and Y. Maeno, Phys. Rev. B **62**, 8725 (2000).
[6] J. S. Lee, Y. S. Lee, T. W. Noh, K. Char, J. Park, S. J. Oh, J.-H. Park, C. B. Eom, T. Takeda, and R. Kanno, Phys. Rev. B **64**, 245107 (2001).
[7] R. S. Perry, L. M. Galvin, A. P. Mackenzie, D. M. Forsythe, S. R. Julian, S. I. Ikeda, and Y. Maeno, Physica B **284**, 1469 (2000).
[8] I. Hase and Y. Nishihara, J. Phys. Soc. Jpn. **66**, 3517 (1997).
[9] S.-I. Ikeda, Y. Maeno, S. Nakatsuji, M. Kosaka, and Y. Uwatoko, Phys. Rev. B **62**, R6089 (2000).
[10] L. Capogna, A. P. Mackenzie, R. S. Perry, S. A. Grigera, L. M. Galvin, P. Raychaudhuri, A. J. Schofield, C. S. Alexander, G. Cao, S. R. Julian, and Y. Maeno, Phys. Rev. Lett. **88**, 076602 (2002).
[11] G. Cao, S. McCall, and J. E. Crow, Phys. Rev. B **55**, R672

(1997).
[12] T. Katsufuji, M. Kasai, and Y. Tokura, Phys. Rev. Lett. **76**, 126 (1996).
[13] M. G. Hildebrand, M. Reedyk, T. Katsufuji, and Y. Tokura, Phys. Rev. Lett. **87**, 227002 (2001).
[14] P. Kostic, Y. Okada, N. C. Collins, Z. Schlesinger, J. W. Reiner, L. Klein, A. Kapitulnik, T. H. Geballe, and M. R. Beasley, Phys. Rev. Lett. **81**, 2498 (1998).
[15] A. V. Puchkov, M. C. Schabel, D. N. Basov, T. Startseva, G. Cao, T. Timusk, and Z.-X. Shen, Phys. Rev. Lett. **81**, 2747 (1998).
[16] J. S. Lee, Y. S. Lee, T. W. Noh, S. Nakatsuji, H. Fukazawa, R. S. Perry, Y. Maeno, Y. Yoshida, S. I. Ikeda, J. Yu, and C. B. Eom, Phys. Rev. B **70**, 085103 (2004).
[17] M. Ortolani, P. Calvani, S. Lupi, P. Maselli, M. Fujita, and K. Yamada, J. Opt. Soc. Am. B **22**, 1994 (2005).
[18] J. S. Lee, S. J. Moon, B. J. Yang, Jaejun Yu, U. Schade, Y. Yoshida, S.-I. Ikeda, and T. W. Noh, Phys. Rev. Lett. **98**, 097403 (2007).
[19] For a review, see T. Timusk and B. Statt, Rep. Prog. Phys. **62**, 61 (1999).
[20] A. F. Santander-Syro, R. P. S. M. Lobo, N. Bontemps, Z. Konstantinovic, Z. Z. Li, and H. Raffy, Phys. Rev. Lett. **88**, 097005 (2002).
[21] M. Ortolani, P. Calvani, and S. Lupi, Phys. Rev. Lett. **94**, 067002 (2005).
[22] A. Toschi, M. Capone, M. Ortolani, P. Calvani, S. Lupi, and C. Castellani, Phys. Rev. Lett. **95**, 097002 (2005).